

Study the effects of TiB₂ reinforcement on the AA-2014 matrix fabricated by friction stir processing

Jitendra Kumar^a, Vipin Kumar Sharma^{*b}, Ajay Partap Singh^c

Department of Mechanical Engineering, IIMT University, Meerut, India

Article Info

Abstract

Article history:

Received 09 Mar 2024

Accepted 11 July 2024

Keywords:

Friction stir processing;

TiB₂;

Aluminum alloy;

Hardness;

Ultimate tensile strength;

Microstructure analysis

This study explores the impact of TiB₂ nanoparticles on the microstructure, microhardness, and tensile properties of AA-2014 surface composite manufactured through Friction Stir Processing (FSP). A series of experiments were conducted with varying FSP parameters, and the findings were compared with the base metal. Microstructure studies revealed optimal bonding between TiB₂ and the AA-2014 substrate at 1200 rpm, surpassing results from 900 and 1600 rpm. However, microstructural analysis unveiled agglomeration of particles and void formation on the composite surface. Microhardness values indicated a substantial increase from 88 HV (AA-2014) to 138 HV (AA-2014/3%TiB₂@1200rpm), attributed to the presence of TiB₂ nanoparticles and FSP-induced modifications. Ultimate Tensile Strength (UTS) values exhibited a noteworthy improvement from 290 MPa (AA-2014) to 465 MPa (AA-2014/3%TiB₂@1200rpm), emphasizing the positive influence of uniform TiB₂ dispersion achieved during FSP. The study underscores the effectiveness of TiB₂ reinforcement and FSP in enhancing the mechanical properties of AA-2014 surface composite, despite observed microstructural features.

© 2024 MIM Research Group. All rights reserved.

1. Introduction

Aluminum alloys have emerged as a superior choice over steel in various industries due to their remarkable strength-to-weight ratio [1]. This characteristic makes aluminum alloys particularly desirable in the aircraft and automotive sectors [2]. In aircraft construction, the utilization of high-strength structural components is essential for ensuring both performance and safety [3]. The 2000 series of aluminum alloys, in particular, has found extensive use in this domain [4]. One of the primary advantages of aluminum alloys, especially those in the 2000 series, is their ability to reduce weight without compromising strength. This weight reduction has a significant impact on fuel efficiency in aircraft, ultimately leading to increased payload capacity [5]. The 2xxx series alloys, such as AA 2014, have become integral in the aerospace industry for achieving these goals [6]. The ongoing trend in favor of aluminum can be attributed to its diverse set of qualities. Not only does it exhibit impressive strength, but it also possesses corrosion resistance, a crucial factor in ensuring the longevity and durability of aircraft [7]. The reduced maintenance and repair costs associated with corrosion-resistant materials further contribute to the economic viability of aluminum alloys in aviation. The various applications of aluminum extend beyond its use in aircraft. The material's reflective, electrically conductive, non-magnetic, non-sparking, and non-combustible properties make it suitable for a wide range of purposes [8]. These characteristics have led to its incorporation in the construction of structural beams, which are vital for the overall integrity of various engineering structures [9]. A notable example of aluminum's versatility is evident in the construction of fuel tanks

*Corresponding author: vipinkumarsharma_me@iimtindia.net

^a orcid.org/0009-0000-0325-1049, ^b orcid.org/0000-0001-5464-8644; ^c orcid.org/0000-0002-7234-4043

DOI: <http://dx.doi.org/10.17515/resm2024.212ma0309rs>

Res. Eng. Struct. Mat. Vol. x Iss. x (xxxx) xx-xx

and booster rockets for both aircraft and space shuttles [10]. The demand for lightweight yet durable materials in these critical components aligns perfectly with the properties offered by aluminum alloys [11]. The lightweight materials not only aid in the efficiency of vehicles but also elevate their general performance and dependability. In the realm of ground transportation, aluminum alloys play a crucial role in the construction of vehicles such as dump trucks, tank trucks, and trailer trucks [12]. The need for robust materials that can withstand the rigors of transportation and hauling is met by aluminum alloys. This usage extends to various industries where the reliability and durability of vehicles are paramount. Within the spectrum of aluminum alloys, the AA 2014 alloy stands out, particularly for its mechanical properties. This alloy is partially composed of copper as its major alloying ingredient, contributing to its strength and other desirable characteristics. In the context of construction, especially in aerospace applications, AA 2014 has become the preferred choice due to its well-balanced properties [13]. Taking the exploration of aluminum alloys further, a recent study involved the use of AA-2014 alloy as a matrix material, reinforced with TiB₂ particles through friction stir processing. This innovative approach aims to enhance the material's mechanical properties and performance in specific applications. The incorporation of reinforcing particles, such as TiB₂, opens up new possibilities for tailoring the properties of aluminum alloys to meet the evolving demands of various industries. In conclusion, the widespread adoption of aluminum alloys, particularly in the 2xxx series, signifies a paradigm shift in material choices for industries where strength, weight, and durability are critical factors [14]. The continuous upward trend in aluminum utilization is justified by its unique combination of properties, including corrosion resistance, non-toxicity, heat conduction, and recyclability [15]. As technology advances, the incorporation of reinforcing particles in aluminum alloys, as demonstrated in the AA-2014 alloy study, showcases the commitment to pushing the boundaries of material science for improved performance and efficiency in construction applications [16]. Whether soaring through the skies or navigating the highways, aluminum alloys have firmly established themselves as indispensable materials in modern engineering and construction [17].

The objective of the study was to investigate the effects of incorporating TiB₂ nanoparticles into AA-2014 aluminum alloy through friction stir processing (FSP) on the bonding quality, microhardness, and ultimate tensile strength (UTS) of the resulting surface composite. The study aimed to assess the optimal processing parameters for achieving good bonding between TiB₂ and the AA-2014 substrate, as well as to analyze the influence of TiB₂ reinforcement on the mechanical properties of the composite material.

2. Materials and Method

2.1. Materials

The choice of aluminum alloys AA-2014 and TiB₂ reinforcement for friction stir processing is driven by their exceptional versatility, making them highly suitable for a diverse range of industries. These alloys have applications in aerospace, automotive, construction, and various other sectors due to their unique combination of properties. The decision to employ friction stir processing reflects the ongoing effort to enhance the mechanical properties of these materials for specific applications. To gain insight into the composition of the chosen alloys, spectrometric analytical equipment was employed.

Table 1. Chemical composition of the AA-2014

Elements	Al	Si	Ti	Cr	Mn	Fe	Cu	Zn	Mg
Wt. %	86.0	0.75	0.23	0.05	0.82	0.30	4.18	0.83	0.83

The resulting chemical composition values are presented in Tables 1 and 2 for AA-2014 and TiB₂ reinforcement, respectively. These nominal values provide a comprehensive understanding of the elemental makeup of each material, laying the foundation for further discussions on their properties and potential applications.

Table 2. Chemical Composition of TiB₂

Reinforcement TiB ₂	Ti	B
Composition	39.78	60.22

2.2. FSP Processing

Friction Stir Processing (FSP) is a specialized technique used to modify the microstructure and properties of metals, particularly aluminum alloys like AA2014 T6. It involves several distinct steps, each carefully orchestrated to achieve desired material properties and structure [18]. The step by step for FSP process is mentioned below:

- Step 1: The process begins with the spindle strategically positioned at the center of the machine. The spindle is then set to rotate at a specific speed, measured in revolutions per minute (rpm). This rotation of the spindle is a crucial initial step in preparing for the subsequent stages of FSP.

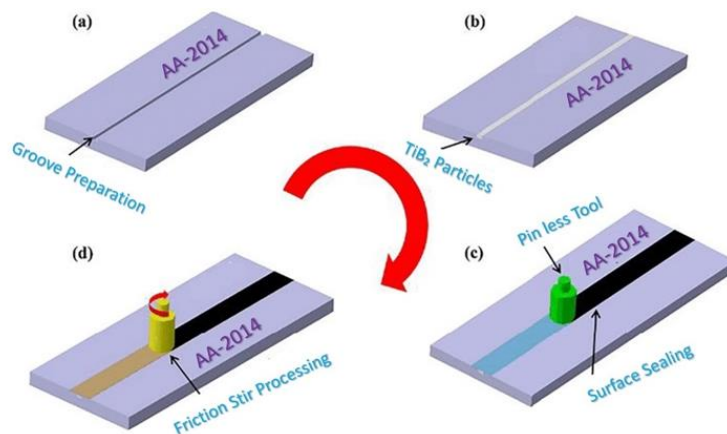


Fig. 1.FSP representation in graphical form

- Step 2: Simultaneously, the machine table undergoes a progressive vertical elevation. This upward movement continues until the tool insert penetrates the surfaces of the aluminum alloy plates by a precise depth, typically around 0.1 mm. This controlled penetration depth is critical as it sets the stage for the material interaction and stirring process [19].
- Step 3: Once the penetration depth is achieved, the spindle remains stationary, spinning in place for a specified duration, typically around 30 seconds. This dwell time serves the purpose of warming the plates in preparation for the welding process. Controlled heating at this stage optimizes the material for subsequent stirring and processing steps [20].
- Step 4: The core of the FSP process lies in the plate mixing procedure, which occurs during this stage. The machine table advances at a defined linear speed, measured in millimeters per minute (mm/min). This movement induces the welding process,

where the rotating tool stirs and mixes the material within its vicinity. The stirring action is crucial for achieving a homogeneous structure and desirable material properties [21].

- Step 5: The combination of the rotational motion of the spindle and the linear movement of the machine table results in a dynamic stirring effect. This intricate process is precisely controlled to ensure uniformity and consistency in the stirred material. The stirring action facilitates the redistribution of alloying elements and the refinement of grain structure, leading to improved mechanical properties [22].
- Step 6: As the machine table progresses and the stirring reaches the specified length of the weld, the retracting step commences. At this point, the forward movement of the tool halts, and it is systematically removed from the sample. This controlled retraction leaves a characteristic hole at the end of the weld. The retracting step is critical as it finalizes the stirring action and shapes the processed material [23].
- Step 7: The hole left at the end of the weld is a consequence of the tool's retraction and serves as a visual marker of the processed region. It provides a clear indication of the extent and location of the FSP treatment [24].
- The FSP process involves a sequence of precisely controlled steps aimed at modifying the microstructure and properties of aluminum alloys through mechanical mixing and stirring. Each step plays a crucial role in achieving the desired material properties and structural characteristics. Table 3 shows the sample nomenclature, processing parameters, and compositions of each specimen.

Table 3. Processing parameters of FSP

Samples Nomenclature	Rotation rate (RPM)	Composition
BM (AA-2014)	1000	100% AA-2014
FSPed-1	900	97%AA-2014- 3%TiB ₂
FSPed-2	1200	97%AA-2014- 3%TiB ₂
FSPed-3	1600	97%AA-2014- 3%TiB ₂

3. Characterization

3.1. Tensile Test

The mechanical characteristics of the treated zone, after heat treatment, were systematically explored through a series of nine experiments. The objective was to assess the impact of heat treatment on these mechanical properties.

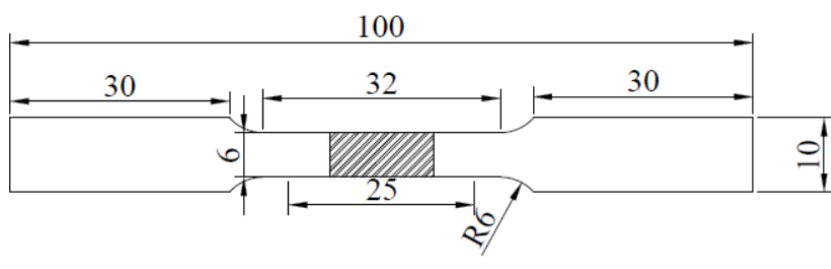


Fig. 2. ASTM Standard E8 for tensile test specimens

The tensile test specimens, crucial for evaluating these properties, were meticulously crafted using CNC wire cut technology. The geometry of these specimens (Figure 2) adhered to the specifications outlined in the ASTM standard E8/E8M-09, specifically designed for sub-size specimens [25].

3.2. Microhardness Testing

The Vickers hardness test, a key method for assessing material hardness, was conducted using a computerized microhardness tester (Melcorp, Model AHT-1000). This modern testing apparatus ensures precision and accuracy in measuring hardness values. The measurements were performed as per ASTM standards, a widely recognized set of guidelines that ensures consistency and comparability of test results [26]. The testing was conducted at several central locations throughout the treated zone, providing a comprehensive understanding of the hardness distribution within the material. This approach allows for the identification of variations in hardness across different regions of the treated zone, providing valuable insights into the impact of the treatment on the material's mechanical properties.

4. Result and Discussions

4.1. Microhardness Evaluation

The microhardness measurements depicted in Figure 3 provide valuable insights into the effects of Friction Stir Processing (FSP) on specimens treated with and without TiB₂ particles at various rotational speeds (900 rpm, 1200 rpm, and 1600 rpm). At a constant traversal speed of 40 mm/min, the figure reveals a trend where increasing the rotational speed often leads to higher microhardness values. This phenomenon is attributed to enhanced dynamic recrystallization; a consequence of the intensified stirring motion induced by the instrument's pin. The microhardness values generally exhibit an upward trend as the rotational speed increases. This suggests that higher rotational speeds contribute to increased hardness in the treated specimens. The intensified stirring motion at elevated speeds is responsible for this effect. Interestingly, the specimens treated with a rotational speed of 1200 rpm demonstrate the highest microhardness values (138 HV) compared to those processed at 1600 rpm and 900 rpm. This highlights an optimal rotational speed for achieving the desired hardness characteristics. Within the stirred zone, the specimen treated at 1200 rpm stands out for having a homogeneous distribution of TiB₂ particles. This results in a uniform scattering of reinforcement throughout the material, contributing to enhanced hardness properties.

The observed increase in microhardness with higher rotational speeds aligns with the concept of dynamic recrystallization. The intensified stirring motion at elevated speeds promotes more effective grain refinement and strengthening mechanisms, leading to enhanced hardness. The optimal microhardness values at 1200 rpm suggest that there is a balance between stirring efficiency and potential material properties. This could be attributed to an ideal combination of heat input, plastic deformation, and particle distribution achieved at this rotational speed.

The homogeneous distribution of TiB₂ particles in the specimen treated at 1200 rpm is crucial. A uniform scattering of reinforcement particles contributes to consistent strengthening effects across the material, resulting in a more homogeneously hardened structure. In conclusion, Figure 3 illustrates the influence of rotational speed on microhardness in FSP-treated specimens, emphasizing the importance of finding an optimal speed for achieving desired material properties. The homogeneous distribution of reinforcement particles further demonstrates the significance of process parameters in tailoring the mechanical characteristics of FSP-treated materials.

The comparative analysis of the microhardness values from this study with other research reveals significant insights into the performance of Friction Stir Processing (FSP) on Al-based alloys. The highest microhardness value in this study, achieved at 1200 rpm with TiB₂ particle reinforcement, is 138 HV. This is substantially higher than the base material

(Al-2014 alloy) which has a hardness of 98 HV. When compared to other studies, such as Gaoqiu Sun et al. on Al7050-TiB₂ (92 HV) [27], and Rajiv Panda et al. on Al2024-TiB₂ (109 HV) [28], the microhardness values from this study indicate a superior improvement in hardness due to the optimal FSP conditions.

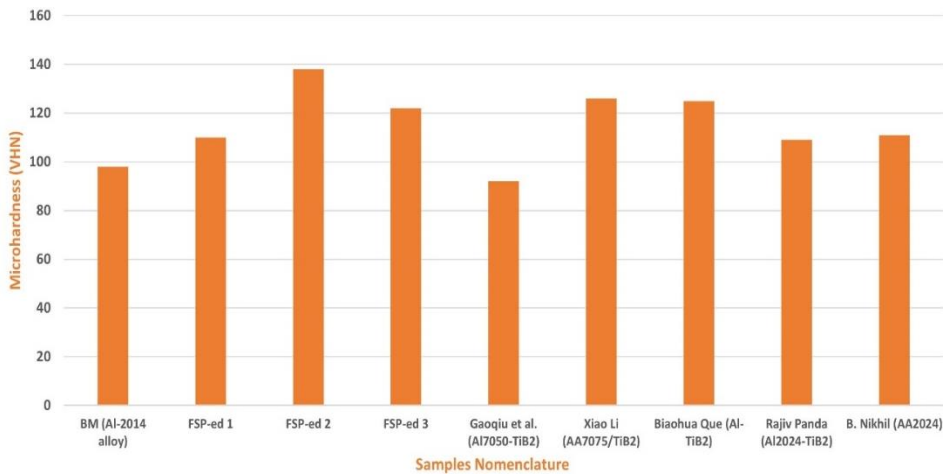


Fig. 3. Hardness values of different FSP-ed specimens

Xiao Li et al. research on AA7075/TiB₂ shows a microhardness of 126 HV [29], and Biaohua Que et al. study on Al-TiB₂ reports 124.9 HV [30], both of which are lower than the 138 HV achieved in the present study. Additionally, B. Nikhil et al. work on AA2024 reveals a microhardness of 111 HV [31], further emphasizing the significant enhancement observed in this study. The superior microhardness at 1200 rpm in this study is attributed to a combination of optimal heat input, plastic deformation, and a homogeneous distribution of TiB₂ particles, which collectively contribute to effective grain refinement and strengthening mechanisms. This comparative analysis underscores the effectiveness of the FSP parameters used in this study, particularly the rotational speed, in achieving enhanced mechanical properties in Al-based alloys reinforced with TiB₂ particles.

4.2. Tensile Strength

The tensile strength characteristics of different specimens (Figure 4) are derived from the base material (BM), which has an initial tensile strength of 290 MPa. The subsequent specimens, FSPed-1, FSPed-2, and FSPed-3, undergo Friction Stir Processing (FSP), resulting in varied tensile strength improvements. Base Material (BM) represents the unprocessed AA-2014 material without any reinforcement or FSP treatment. The tensile strength for base material was noted as 290 MPa. The specimen FSPed-1 after FSP treatment involves mixing and recrystallizing the base material, leading to a significant tensile strength improvement from 290 MPa to 360 MPa. The addition of TiB₂ particles, coupled with the stirring process, likely contributes to increased dislocation density and refined grain size in the microstructure, resulting in improved strength. Further processing enhances the tensile strength compared to FSPed-1, FSPed-2 has tensile strength of 465 MPa. Additional FSP treatment might cause more homogenization of TiB₂ particles in the matrix, leading to further strengthening. FSPed-3 exhibits the highest tensile strength (405 MPa) among the specimens. Continued processing may have caused even more refinement of the microstructure and further dispersion and alignment of TiB₂ particles, resulting in the highest tensile strength. The progressive increase in tensile strength from FSPed-1 to FSPed-3 indicates the cumulative effect of multiple FSP

treatments on the mechanical properties of the material. The addition of TiB_2 particles and the stirring process during FSP play crucial roles in enhancing dislocation density, refining grain size, and promoting homogenization, leading to improved tensile strength. The highest tensile strength in FSPed-2 suggests that continued processing results in further microstructural refinement and better dispersion and alignment of TiB_2 particles, contributing to the material's strength.

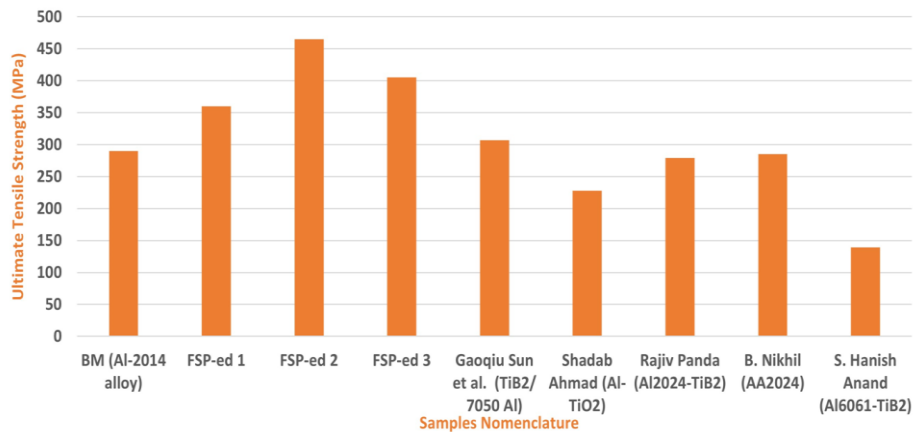


Fig. 4. UTS values of different FSP-ed specimens

Comparatively, the tensile strengths reported in other studies also provide insights into the effectiveness of different reinforcement particles and base materials. Gaoqiu Sun et al. achieved a tensile strength of 307 MPa with $\text{TiB}_2/7050$ Al [27], which is notable but lower than the FSPed-2 and FSPed-3 specimens from this study. Shadab Ahmad et al. work on Al- TiO_2 reported a tensile strength of 228 MPa [32], indicating that TiO_2 reinforcement, while beneficial, may not be as effective as TiB_2 in enhancing tensile strength. Rajiv Panda et al. study on Al2024- TiB_2 shows a tensile strength of 279 MPa [28], and B. Nikhil et al. work on AA2024 reports a tensile strength of 285 MPa [31]. Both values are lower than those achieved in the present study, suggesting that the specific FSP conditions and the base material (AA-2014) used in this research might be more conducive to tensile strength improvement. S. Hanish Anand et al. research on Al6061- TiB_2 reports a tensile strength of 139 MPa [33], which is the lowest among the studies considered. This further emphasizes the superior tensile strength achieved through the optimized FSP conditions and TiB_2 reinforcement in the current study.

4.3. Microstructure Analysis

The microstructure analysis is crucial in understanding the distribution and arrangement of TiB_2 nanoparticles within the AA-2014 alloy, providing insights into how these factors influence the material's mechanical properties. The base material, representing unprocessed AA-2014, serves as the control in this study. The FSPed-2 specimen, reinforced with 3% TiB_2 nanoparticles, showcases a significant improvement in the dispersion of these reinforcing particles within the AA-2014 matrix. The enhanced dispersion of TiB_2 nanoparticles in the FSPed-2 specimen is a key contributor to its improved mechanical properties. This is because a more uniform distribution of TiB_2 particles leads to better interfacial bonding between the matrix and the nanoparticles. Such improved bonding facilitates effective load transfer from the softer aluminum matrix to the harder TiB_2 particles, thereby enhancing the overall strength and hardness of the material. Additionally, the fine and uniform dispersion of TiB_2 particles helps in refining

the grain structure of the aluminum matrix. This grain refinement is a result of dynamic recrystallization promoted by the FSP process, which further contributes to the enhancement of mechanical properties such as tensile strength and hardness.

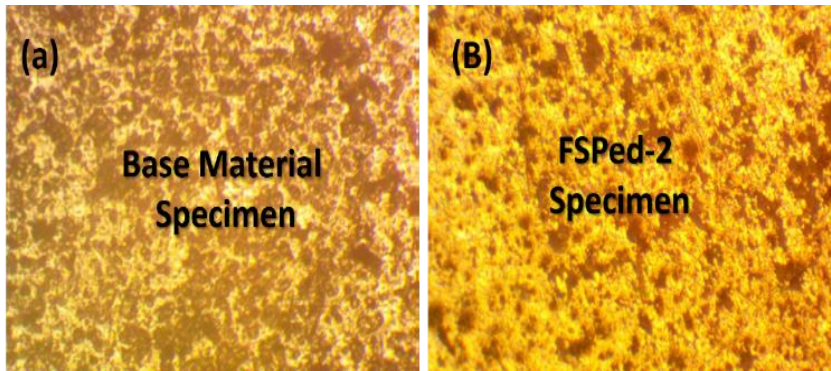


Fig. 5. Microstructure of BM and FSPed-2 specimens

In Figure 5, the mechanical properties of the FSPed-2 specimen, including tensile strength and hardness, are compared to those of the base material. The tensile strength of the FSPed-2 specimen shows a marked increase, attributed to the better dispersion of TiB_2 nanoparticles. This uniform distribution not only strengthens the material but also improves its ductility by preventing the formation of weak points that could lead to fracture. The hardness of the FSPed-2 specimen is also significantly higher than that of the base material, which can be explained by the Hall-Petch effect, where the fine grain structure and the presence of hard particles hinder the movement of dislocations, thereby increasing the material's resistance to deformation. The interaction between the TiB_2 nanoparticles and the aluminum matrix is a critical aspect of the material's enhanced properties. Previous research has shown that TiB_2 particles serve as effective barriers to dislocation movement, contributing to the strengthening of the material through mechanisms such as Orowan strengthening, where the dislocations bypass the nanoparticles, and grain boundary strengthening, where the fine grains enhance the yield strength of the material. Yihong Wu et al. revealed that the deagglomeration and dispersion of TiB_2 particles improve both the strength and ductility of the particulate-reinforced aluminum matrix composite. The uniform distribution of precipitates and the elimination of agglomerated TiB_2 bumps and residual Al_3Ti blocks are crucial for these improvements [34]. Santha Rao et al. observed that the microstructural analysis sheds light on the intricate mechanisms during the FSP process. The uniform distribution of filler particles in the stir zone contributes to improved mechanical properties and signifies the effectiveness of the welding conditions, particularly at higher rotational speeds. The nuanced interplay between mixing, distribution of filler particles, recrystallization, and grain refinement underscores the complexity of the microstructural evolution in the fabrication of composites [35].

5. Conclusion

The fabrication of AA-2014 TiB_2 surface composite using the FSP process has been accomplished. This composite has numerous industrial applications, particularly in the automotive, aerospace, and construction sectors, owing to its enhanced mechanical properties and durability. The investigation into the effect of TiB_2 particles on the microstructure, microhardness, and tensile behavior of AA-2014 surface composite fabricated by Friction Stir Processing (FSP) has yielded significant conclusions.

- The optimal bonding of TiB₂ with the AA-2014 substrate was consistently observed at 1200 rpm, as evidenced by good bonding compared to both the base metal and FSP-ed specimens processed at 900 and 1600 rpm. This optimal bonding at 1200 rpm is critical as it ensures the effective integration of TiB₂ particles within the AA-2014 matrix, enhancing the overall properties of the composite.
- Microhardness values for AA-2014 and AA-2014/3%TiB₂ @1200rpm surface composite were measured at 88 HV and 138 HV, respectively. The significant increase in hardness value is attributed to the presence of TiB₂ nanoparticles and the modifications induced by the FSP process. The incorporation of TiB₂ particles into the AA-2014 matrix results in a harder surface, which is indicative of enhanced strength and resistance to deformation, showcasing the effectiveness of the TiB₂ reinforcement.
- Ultimate tensile strength (UTS) values for AA-2014 and AA-2014/3%TiB₂ @1200rpm surface composite were found to be 290 MPa and 465 MPa, respectively. The substantial increase in UTS is linked to the uniform dispersion of TiB₂ nanoparticles within the matrix material (AA-2014 alloy) during the FSP process. This uniform dispersion of TiB₂ particles not only enhances the load-bearing capacity of the composite but also improves its overall tensile behavior.

The addition of TiB₂ particles and the optimal processing parameters of FSP at 1200 rpm significantly improve the microhardness and tensile strength of the AA-2014 alloy. The enhanced properties are attributed to the uniform dispersion and strong bonding of TiB₂ particles within the matrix, resulting in a surface composite with superior mechanical properties compared to the unreinforced AA-2014 alloy and those processed at different rpm settings. These findings underscore the potential of TiB₂-reinforced AA-2014 composites for applications necessitating high strength and hardness.

Nomenclature

FSP AMMCs	Friction Stir Processing Aluminum metal matrix composites	BM AA-2014	Base Material Aluminum 2014 Alloy
AS	Advanced Side	TiB ₂	Titanium Diboride
RS	Retreating Side	TiO ₂	Titanium Dioxide
TMAZ	Thermo-Mechanically Affected Zone	UTS	Ultimate Tensile Strength
HAZ	Heat Affected Zone	VHN	Vickers Hardness

References

- [1] Vipin S, Sharma K. A review of recent research on rare earth particulate composite materials and structures with their applications. *Trans Indian Inst Met.* 2021. <https://doi.org/10.1007/s12666-021-02338-y>
- [2] Sharma VK, Kumar V, Joshi RS. Experimental investigation on effect of RE oxides addition on tribological and mechanical properties of Al-6063 based hybrid composites. *Mater Res Express.* 2019;6(8). <https://doi.org/10.1088/2053-1591/ab2504>
- [3] Kumar D, Angra S, Singh S. Synthesis and characterization of DOE-based stir-cast hybrid aluminum composite reinforced with graphene nanoplatelets and cerium oxide. 2023. <https://doi.org/10.1108/AEAT-04-2023-0104>
- [4] Kumar S, Kumar R, Goyal KK, Sharma N. Experimental study on tensile strength of Al2024/SiC/FA/Graphite hybrid MMC prepared by stir casting. *Mater Today Proc.* 2022;395-399. <https://doi.org/10.1016/j.matpr.2022.03.306>
- [5] Alderliesten R, Open Textbook Library. Introduction to aerospace structures and materials. 2018. <https://doi.org/10.5074/T.2018.003>

- [6] Srivastava AK, Maurya NK, Maurya M, Dwivedi SP, Saxena A. Effect of multiple passes on microstructural and mechanical properties of surface composite Al 2024/SiC produced by friction stir processing. *Ann Chim Sci Mat.* 2020;44(6):421-426. <https://doi.org/10.18280/acsm.440608>
- [7] Kumar D, Angra S, Singh S. Investigation of corrosion behavior of stir-cast hybrid aluminum composite reinforced with CeO₂ and GNPs nanoparticles. 2023;59(6):1210-1218. <https://doi.org/10.1134/S2070205123701186>
- [8] Iranshahi F, Nasiri MB, Warchomicka FG. Investigation of the degradation rate of electron beam processed and friction stir processed biocompatible ZKX50 magnesium alloy. *J Magnes Alloy.* 2022;10(3):707-720. <https://doi.org/10.1016/j.jma.2021.08.016>
- [9] You X, et al. A review of research on aluminum alloy materials in structural engineering. *Dev Built Environ.* 2024;17(September 2023):100319. doi:10.1016/j.dibe.2023.100319. <https://doi.org/10.1016/j.dibe.2023.100319>
- [10] Lorusso M, Aversa A, Marchese G, Calignano F, Manfredi D, Pavese M. Understanding friction and wear behavior at the nanoscale of aluminum matrix composites produced by laser powder bed fusion. *Adv Eng Mater.* 2020;22(2):1-12. <https://doi.org/10.1002/adem.201900815>
- [11] Kale SS, Raja VS, Bakare AK. Enhancing the environmentally assisted cracking resistance of aircraft quality Al alloy of type AA7075 stiffened with polymer matrix composite using cerium chloride inhibitor. *Trans Indian Inst Met.* 2018;71(12):3021-3027. <https://doi.org/10.1007/s12666-018-1403-z>
- [12] Abraham CB, Nathan VB, Jaipaul SR, Nijesh D, Manoj M, Navaneeth S. Basalt fibre reinforced aluminium matrix composites - a review. *Mater Today Proc.* 2020;21:380-383. <https://doi.org/10.1016/j.matpr.2019.06.135>
- [13] Chak V, Chattopadhyay H, Dora TL. A review on fabrication methods, reinforcements and mechanical properties of aluminum matrix composites. *J Manuf Process.* 2020;56(May):1059-1074. <https://doi.org/10.1016/j.jmapro.2020.05.042>
- [14] Partheeban CMA, Rajendran M, Vettivel SC, Suresh S, Moorthi NSV. Mechanical behavior and failure analysis using online acoustic emission on nano-graphite reinforced Al6061-10TiB₂ hybrid composite using powder metallurgy. *Mater Sci Eng A.* 2015;632:1-13. <https://doi.org/10.1016/j.msea.2015.02.064>
- [15] Paper R. Lignocellulosic abaca fibre-reinforced thermoplastic composites as future sustainable structural materials: a bibliometric analysis and literature review. 2024.
- [16] Kumar S, Alok N, Sisir S. Impact of process parameters on solid particle erosion behavior of waste marble dust-filled polyester composites. *Arab J Sci Eng.* 2021;46(8):7197-7209. <https://doi.org/10.1007/s13369-020-05175-1>
- [17] Kalhapure M, Dighe P. Impact of silicon content on mechanical properties of aluminum alloys. *Int J Sci Res (IJSR).* 2013;14(6):2319-7064.
- [18] Khyavi BA, Aghchai AJ, Arbabtafti M, Kazem M, Givi B. Effect of friction stir processing on mechanical properties of surface composite of Cu reinforced with Cr particles. 2014;829:851-856. <https://doi.org/10.4028/www.scientific.net/AMR.829.851>
- [19] Raja R, et al. Development of Al-Mg₂Si alloy hybrid surface composites by friction stir processing: mechanical, wear, and microstructure evaluation. *Mater.* 2023;16:4131. <https://doi.org/10.3390/ma16114131>
- [20] Ajenifuja E, Odetola P, Popoola API, Popoola O. Spark plasma sintering and structural analysis of nickel-titanium/coconut shell powder metal matrix composites. *Int J Adv Manuf Technol.* 2020;108(11-12):3465-3473. <https://doi.org/10.1007/s00170-020-05634-x>
- [21] Siddesh Kumar NM, Sadashiva M, Monica J, Praveen Kumar S. Investigation on corrosion behaviour of hybrid aluminium metal matrix composite welded by friction stir welding. *Mater Today Proc.* 2021;52:2339-2344. <https://doi.org/10.1016/j.matpr.2022.01.362>

- [22] Singh S, Pal K. Influence of texture evolution on mechanical and damping properties of SiC/Li₂ZrO₃/Al composite through friction stir processing. *J Eng Mater Technol Trans ASME*. 2020;142(2):1-9. <https://doi.org/10.1115/1.4045495>
- [23] Kumar S, Kumar A, Vanitha C. Corrosion behaviour of Al 7075/TiC composites processed through friction stir processing. *Mater Today Proc*. 2019;15:21-29. <https://doi.org/10.1016/j.matpr.2019.05.019>
- [24] Zhang Z, Wu Q. Numerical studies of tool diameter on strain rates, temperature rises and grain sizes in friction stir welding. *J Mech Sci Technol*. 2015;29(10):4121-4128. <https://doi.org/10.1007/s12206-015-0906-3>
- [25] Xia J, Lewandowski JJ, Willard MA. Tension and fatigue behavior of Al-2124A/SiC-particulate metal matrix composites. *Mater Sci Eng A*. 2020;770(June 2019):138518. <https://doi.org/10.1016/j.msea.2019.138518>
- [26] Venkatesan SP, Muthuswamy G, Shyam Sundar R, Ganesan S, Hemanandh J. Investigation of mechanical properties of aluminum metal matrix composites with nanomaterial reinforcement. *Mater Today Proc*. 2022;62:572-582. <https://doi.org/10.1016/j.matpr.2022.03.594>
- [27] Sun G, Zhao G, Shao L, Li X, Deng Y. Particle dispersion and mechanical properties enhancement of in-situ TiB₂/7050 Al matrix composite via additive friction stir deposition. *Mater Lett*. 2024;357(November 2023):135790. <https://doi.org/10.1016/j.matlet.2023.135790>
- [28] Panda R, Gupta RK, Mandal A, Chakravarthy P. Processing, microstructure evolution, and heat treatment response of AA2024 and its metal matrix composites of in situ TiB₂ dispersoids. *J Mater Eng Perform*. 2024. <https://doi.org/10.1007/s11665-024-09344-3>
- [29] Li X, et al. Exceptional strength and wear resistance in an AA7075/TiB₂ composite fabricated via friction consolidation. *Mater Des*. 2024;242(March):113006. <https://doi.org/10.1016/j.matdes.2024.113006>
- [30] Que B, Chen L, Chen Y, Qian L, Zhao G, Zhang C. Fabrication of Al/Al-TiB₂ laminate composites via hot press sintering process: an insight into the mechanical properties and fracture behavior. *J Manuf Process*. 2024;109(July 2023):53-64. <https://doi.org/10.1016/j.jmapro.2023.11.040>
- [31] Nikhil B, Govindan P. Effect of tool probe geometry on the material flow and mechanical behaviour of dissimilar AA2024/AA7075 friction stir welded joints. *Int J Interact Des Manuf (IJIDeM)*. 2024;18(3):1645-1664. <https://doi.org/10.1007/s12008-023-01717-7>
- [32] Ahmad S, et al. Experimental studies on mechanical properties of Al-7075/TiO₂ metal matrix composite and its tribological behaviour. *J Mater Res Technol*. 2024;30(May):8539-8552. <https://doi.org/10.1016/j.jmrt.2024.05.227>
- [33] Anand SH, Sathishkumar NVB. Microstructural, mechanical and tribological analysis of TiB₂ ceramic-reinforced Al6061 aluminium alloy composites. *Arab J Sci Eng*. 2024;49(2):1827-1842. <https://doi.org/10.1007/s13369-023-07978-4>
- [34] Wu Y, Li L, Kang H, Guo E, Li J, Du G. Agglomerating behavior of in-situ TiB₂ particles and strength-ductility synergetic improvement of in-situ TiB₂p/7075Al composites through ultrasound vibration. *Mater Charact*. 2024;208(September 2023):113652. <https://doi.org/10.1016/j.matchar.2024.113652>
- [35] Dakarapu SR, Chinta ND, Reddy S, Avinash K, Shaik K, Chakravarthy P. Optimization of process parameters for improvement of joint strength of dissimilar aluminum alloys by friction stir welding with an activated flux of titanium diboride. *Int J Interact Des Manuf (IJIDeM)*. 2024. <https://doi.org/10.1007/s12008-024-01787-1>